Adsorption mechanisms, structures, and growth regimes of an archetypal self-assembling system: Decanethiol on Au(111)

F. Schreiber* and A. Eberhardt†
Princeton Materials Institute, Princeton University, Princeton, New Jersey 08544

T. Y. B. Leung
Princeton Materials Institute, Princeton University, Princeton, New Jersey 08544
and Department of Chemistry, Princeton University, Princeton, New Jersey 08544

P. Schwartz
Princeton Materials Institute, Princeton University, Princeton, New Jersey 08544

S. M. Wetterer and D. J. Lavrich
Princeton Materials Institute, Princeton University, Princeton, New Jersey 08544
and Department of Chemistry, Princeton University, Princeton, New Jersey 08544

L. Berman
National Synchrotron Light Source, Brookhaven National Laboratory, Upton, New York 11973

P. Fenter‡ and P. Eisenberger§
Princeton Materials Institute, Princeton University, Princeton, New Jersey 08544

G. Scoles
Princeton Materials Institute, Princeton University, Princeton, New Jersey 08544
and Department of Chemistry, Princeton University, Princeton, New Jersey 08544
(Received 24 November 1997)

We present a study using several techniques of the growth of decanethiol monolayers deposited on single-crystal gold surfaces. Through independent measurements of coverage, energetics, and structure as a function of the growth rate and temperature, we provide a quantitative, in-depth description of the *molecular* processes by which these aliphatic molecules ''self-assemble'' into highly ordered structures in the absence of a solvent. We find that the multiple-energy scales present in these systems produce distinct adsorption mechanisms, structures, and growth regimes, indicating a complexity that is likely to be a general characteristic of this broad class of self-assembling systems. [S0163-1829(98)03019-7]

Self-assembly is a widely observed phenomenon in natural systems,[1] and is also a materials processing route by which materials with ''predesigned'' functions and length scales can be formed through the self-organizing tendencies of the molecular components.[2] As such, it is a potentially important method in materials science providing a flexible alternative to lithography as a versatile technique for the creation of novel materials.[3] Monolayers of long chain molecules self-assembled on single-crystalline surfaces (SAM's) (Refs. 4 and 5) are ideal systems to study the process of molecular self-organization from a fundamental perspective. This class of materials contains most of the characteristics common to other self-organizing systems, such as cell membranes and Langmuir monolayers (e.g., asymmetric interfacial binding, a large number of conformational degrees of freedom, and the important presence of van der Waals interactions). At the same time, the presence of a crystalline substrate provides the stability required for growth studies where the system's structure can be quantitatively characterized. While much is known about the many structures that SAM's adopt,[4–8] relatively little is known at the molecular level about the *assembly process*.[9,10] Equally little is known about the degree to which these processes reflect thermodynamic vs nonequilibrium behavior, since most previous quantitative growth studies have used either ''macroscopic'' or *indirect* (i.e., spectroscopic) probes of the growth process.[11–15]

In this work we synthesize the results obtained with diffraction-based techniques, which provide a direct and quantitative measure of the evolution of structure and order, with independent measurements of coverage and adsorption energetics to provide a comprehensive description of the processes involved in self-assembly. We have chosen to study decanethiol $[CH_3(CH_2)_9SH$, or C10] on Au(111) surfaces since it is one of the most thoroughly characterized SAM systems,[4,6,8,16,17] and therefore represents one of the best opportunities for a quantitative understanding of the equilibrium and kinetic aspects of the self-assembly process.

We have chosen to grow the films in ultrahigh vacuum via vapor phase deposition[7,8,10] since this allows us to follow the molecular-level growth process *in situ* with a range of complementary techniques including grazing incidence x-ray

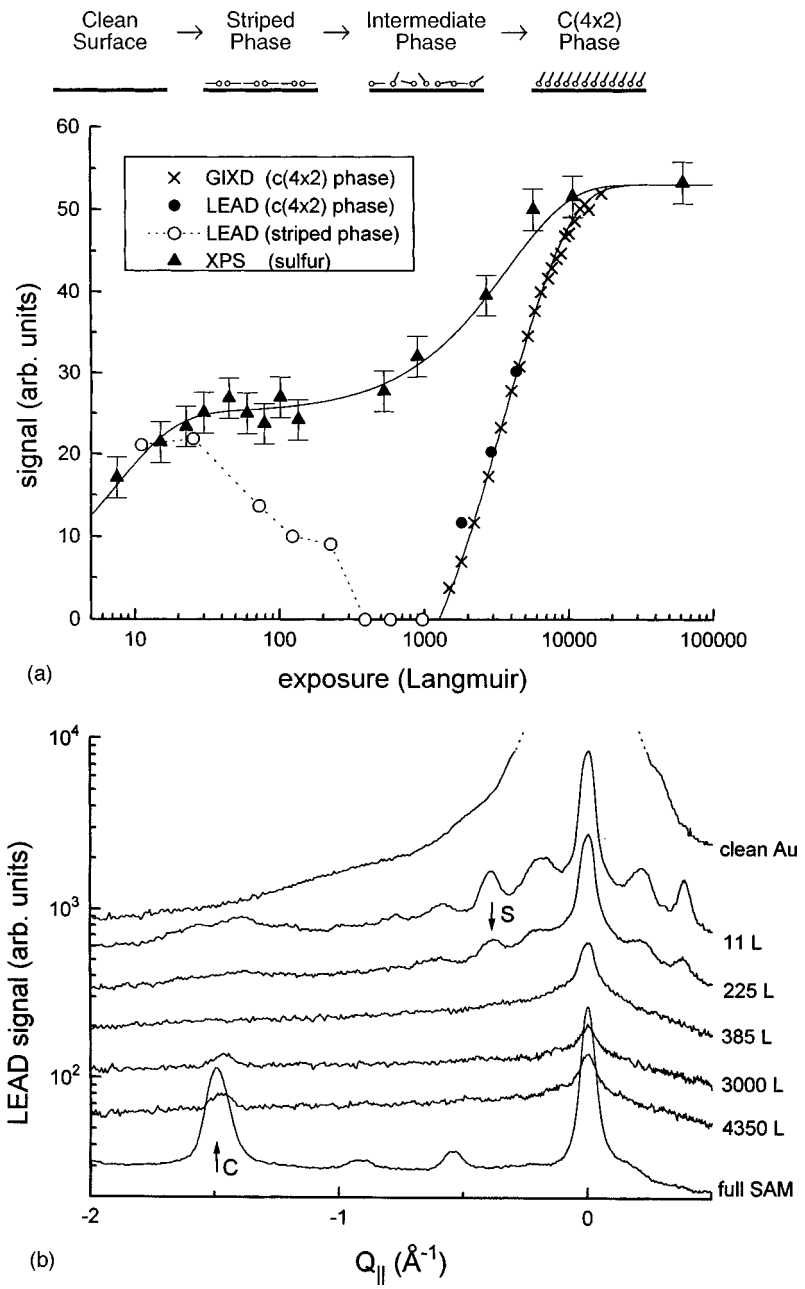

FIG. 1. (a) The vapor phase deposition of decanethiol on Au(111) is shown through XPS, LEAD, and GIXD at 25 °C. The XPS data ($h\nu = 3136$ eV) reflect both changes in the C10 coverage and the attenuation through the hydrocarbon layer (when the hydrocarbon chain ''stands up'' in the IP and C phases) through the $S(1s)$ photoelectron peak ($E_b = 2472$ eV). The GIXD and LEAD data show the integrated intensity of the striped and $C(4\times2)$ diffraction peaks found at $Q_{\|} = 0.40$ and 1.452 Å^{-1}, respectively. The resulting structural evolution is shown in the schematic. (b) Evolution of the LEAD diffraction spectra vs exposure. The Bragg peaks noted by S (striped) and C [$C(4\times2)$] were used in (a). No diffraction is observed in the LEAD data for exposures between ~300 and ~1000 L.

diffraction (GIXD), low energy He atom diffraction (LEAD), He atom reflectometry (HAR), and x-ray photoelectron spectroscopy (XPS). The GIXD and XPS measurements were performed at the X10B and X24A beamlines, respectively, at the National Synchrotron Light Source. We use well-characterized single-crystal Au(111) substrates[8,9] since we are interested in understanding the intrinsic behavior of the system. The close similarity in the growth properties as determined by the x-ray and He atom based techniques (the latter being *entirely* nondestructive) demonstrates that none of the behavior discussed below is affected by x-ray exposure.

To provide an overview of the growth processes, in Fig. 1 we follow the evolution of a C10 monolayer adsorbed from the vapor phase (at room temperature), through four orders of magnitude of thiol exposures.[18] XPS data of the evolution of the S-$K(1s)$ photoelectron yield [Fig. 1(a)] demonstrate that the adsorption of C10 is well-described by a two-stage process in which an initial monolayer phase is rapidly formed, followed by a much slower evolution to monolayer completion.[19] Parallel measurements (not shown) of the evolution of the Au-$M_{\rm v}(3d_{5/2})$ photoelectron yield exhibit a similar evolution, but in which the photoelectron yield decreases at each of the two stages of growth. Together, these

data clearly demonstrate that the observed adsorption process is driven by the evolution of molecular *coverage* and is not an artifact of changes in the molecular orientation or conformation. Fitting these data to a two-step Langmuir kinetics of the form $A_1\exp(-t/\tau_1)+A_2\exp(-t/\tau_2)$, we find that $\tau_1 = 7.2$ L and $\tau_2 = 3750$ L.

Low-energy atom diffraction (LEAD) data in Fig. 1(b) demonstrate that the structure following the first rapid adsorption process (τ_1) is that of a ''striped'' phase (having an $11\times\sqrt{3}$ unit mesh), which has been observed to be the stable low coverage phase at room temperature.[6,8] In this phase, the molecular axis is believed to lie flat on the Au(111) surface, having an ideal coverage of 0.27 ML (1 ML $=4.6\times10^{14}$ mol/cm^2). At higher exposures, both GIXD and LEAD reveal that the second, $\sim$500 times slower, time constant (τ_2) is associated with the formation of the denser (''standing up'') phase, a $C(4\times2)$ superlattice of the close packed hexagonal $(\sqrt{3}\times\sqrt{3})R30°$ structure. This phase nucleates and grows with a Langmuir-like evolution to completion ($\Theta = 1$ ML), as is evident in the XPS, GIXD, and LEAD data. It might be expected that the $C(4\times2)$ phase would form for any coverage exceeding the ideal striped coverage (0.27 ML). Instead, the LEAD data clearly show that the striped phase disorders as the exposure is increased above $\sim$300 L, and that the $C(4\times2)$ phase nucleates only for exposures of >1000 L. That is, adsorption beyond the striped phase's ideal coverage (0.27 ML) apparently disrupts the molecular order of the stripes [as has been independently observed with STM (Ref. 10)], but is insufficient to induce the nucleation of the denser $C(4\times2)$ phase. This suggests that additional structures may coexist at intermediate coverages between the striped and $C(4\times2)$ phases,[20] which, for simplicity, we refer to as the ''intermediate'' phase (IP).

There has been discussion in the literature concerning long term reorganization processes,[21] in which it is believed that the time scale for *molecular organization* (e.g., removal of gauche defects from the hydrocarbon chains) is significantly longer than the time scale for *adsorption*, as has been reported for the longer chain length C22/Au(111) system. By independently measuring both the coverage and structure during monolayer evolution, we find that the evolution of the system studied here, C10/Au(111), is instead described as a series of well-defined *transitions* as a function of coverage (see also the discussion of phase behavior below). Consequently, the coverage evolves through the coexistence of discrete phases, and *not* through a continuous variation in the local monolayer structure (e.g., the tilt angle). Furthermore, real-time kinetic measurements[9] clearly show that the monolayer evolution in the coverage range of $0.47\leqslant\Theta\leqslant1.0$ ML (where these long term reorganization processes are expected to be observed[21]) can be described by a single temperature-dependent growth rate (even at relatively fast growth rates and low substrate temperatures, where it might be expected that the rate of internal organization might become slower than the adsorption rate).[9] Therefore, we find no evidence that long term reorganization is an intrinsic characteristic of the vapor phase growth of C10/Au(111).

A key to understanding the monolayer evolution during growth can be found through the adsorption thermodynamics as a function of chain length, n. Using He atom reflectometry as a surface specific probe of the coverage as a function of temperature, we have measured the systematic variation of the physisorption and chemisorption energies (E_{ph} and E_{ch}, respectively) of thiols and alkanes on Au(111).[22] In Fig. 2(a), we show a typical HAR-detected thermal desorption spectrum for C8/Au(111) in the low coverage regime. The data clearly show two peaks demonstrating the presence of two distinct adsorption states. While a full description of the adsorption thermodynamics will be presented elsewhere,[22] the systematic variation of these data as a function of hydrocarbon chain length [Fig. 2(b)] clearly shows that the higher-temperature desorption peak in Fig. 2(a) is independent of the chain length [solid line, Fig. 2(b)] and therefore can be associated with the strength of the S-Au bond of the *chemisorbed* species. In contrast, the lower-temperature peak depends linearly with chain length as expected for a *physisorbed* species [dotted line, Fig. 2(b)]. This interpretation is

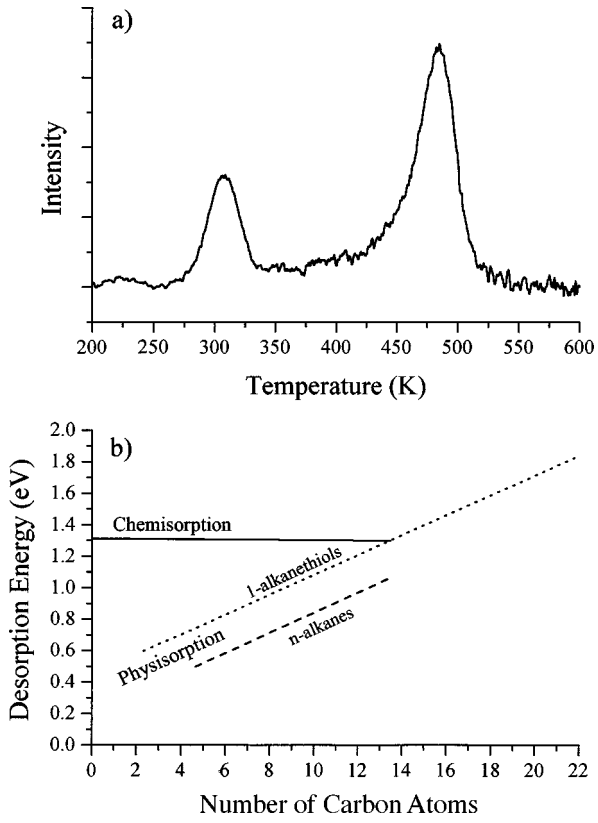

FIG. 2. (a) Temperature programmed desorption (TPD) of C8/Au(111) as measured by He atom reflectometry (HAR). Upon thermal desorption of an adsorbed molecule, the raw HAR signal increases in a stepwise fashion (due to the high surface specular reflectivity of the bare gold surface). The data shown are the derivative of the raw HAR signal as a function of temperature, which are directly comparable to traditional TPD data. The data clearly exhibit two distinct desorption peaks at $T_{ph} = 310$ K and $T_{ch} = 480$ K, due to desorption of the physisorbed and chemisorbed species, respectively. (b) The chainlength dependence of the n-alkyl thiol and n-alkane desorption energies [derived from data similar to those in (a)]. The lines are a best fit to data for a range of chain lengths ($2\leqslant n\leqslant22$ for thiols and $6\leqslant n\leqslant12$ for alkanes). The chemisorption energy is found to be constant over the measured range, while the physisorption energy depends linearly upon the hydrocarbon chainlength, n. The full details of this technique and the data processing are described in Ref. 22.

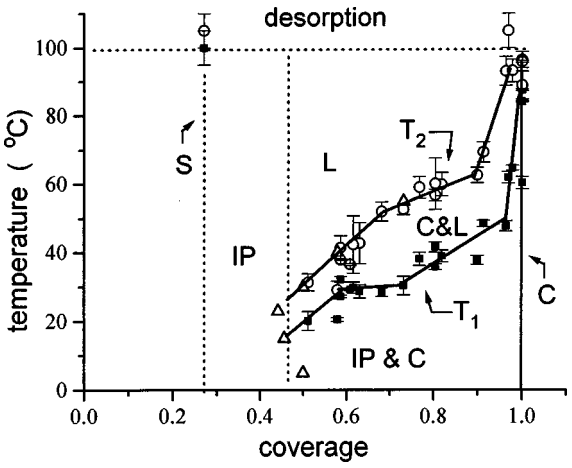

FIG. 3. The coverage-temperature (Θ,T) phase diagram of C10/Au(111) derived by GIXD. The phases include the striped (S), the intermediate (IP), the $C(4\times2)$ (C), and the melted (L) phases, respectively, with the vertical lines indicating the nominal coverages of the striped phase (0.27 ML), the nucleation of the $C(4\times2)$ phase (0.47 ML), and saturation of the $C(4\times2)$ phase (1 ML). The filled squares and open circles denote the temperatures at which melting begins (T_1) and is completed (T_2), respectively, as determined by melting experiments. $T_2(\Theta)$ is also determined through the onset of the $C(4\times2)$ phase in kinetic real-time measurements (open triangles) during growth.

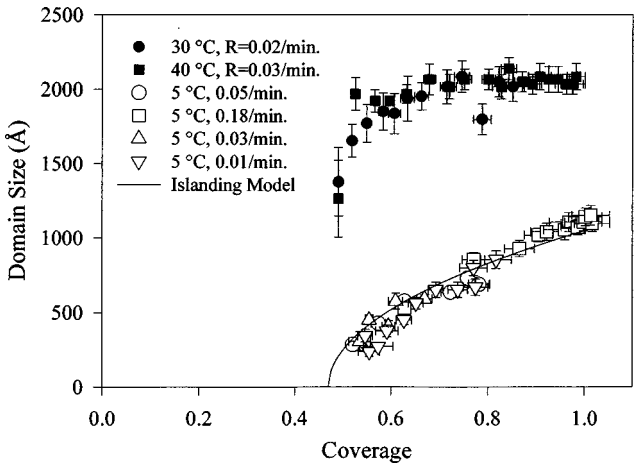

FIG. 4. The domain size as a function of the C10 coverage through *in situ* GIXD measurements during growth, for a range of temperatures and growth rates (inset), where the growth rate R is the inverse of the second time constant, τ_2, described in the text. The solid line is calculated assuming that growth is via a fixed number of islands whose size increases monotonically.

confirmed by the dashed line [Fig. 2(b)], which is the measured dependence of the desorption energy for simple alkane molecules (which only physisorb). For C10, we find that these desorption energies are $E_{\rm ph}=1.1\pm0.05$ eV and $E_{\rm ch}=1.28\pm0.05$ eV, which show that both of these molecule-substrate interactions are significantly stronger than the intermolecular interactions (e.g., the bulk heat of vaporization is 0.68 eV). They also demonstrate a unique characteristic of this system: the *physisorption* energy, which is generally expected to be weak (and is proportional to the hydrocarbon chainlength), is actually comparable to the *chemisorption* energy for chain lengths above $n=10$.

In view of the above, at the initial stage of growth (τ_1) the physisorbed phase in contact with bare Au at room temperature will quickly saturate, and therefore the coverage of physisorbed molecules will be insensitive to changes in pressure and temperature. We believe that these physisorbed molecules then convert to the chemisorbed state, resulting in the observed striped phase (see Fig. 1). In the second stage of growth (τ_2), using GIXD and LEAD we have found that the formation of the $C(4\times2)$ phase is a physisorption mediated process,[9] which we believe is due to a second, more weakly bound, physisorbed precursor that exists in the presence of the chemisorbed striped phase.

Having demonstrated that multiple phases are present in the growth process, we now address the relationship between the equilibrium phase behavior and the evolution of order during growth. A systematic exploration of the coverage-temperature (Θ,T) phase diagram (see Fig. 3) can be obtained using GIXD through both *equilibrium* measurements (as a function of temperature at a given coverage) and real-time *kinetic* measurements (as a function of exposure at a given temperature). In order to convert the experimental exposure to coverage, we have made use of the simple proportionality between the GIXD integrated intensity and the coverage of a given phase [in this case the $C(4\times2)$ phase],[23] the observation of two-time constants in the XPS data (Fig. 1), and the more extensive data on the adsorption kinetics described elsewhere.[9] We find excellent agreement between the phase boundaries as derived through the kinetic and equilibrium measurements, which implies that these results reflect the *intrinsic* behavior of the system.

From the (Θ,T) phase diagram in Fig. 3, we see that the coverage at nucleation of the $C(4\times2)$ phase is 0.47 ML. Since the ideal coverage of the striped phase is 0.27 ML, this further supports the notion of an additional ''intermediate'' phase(s) prior to nucleation of the $C(4\times2)$ phase (see Fig. 1). These data also show that the melting temperature of the $C(4\times2)$ phase depends strongly and nonmonotonically upon the coverage: while the complete monolayer $(\Theta=1$ ML) begins to melt at ~90 °C, the melting temperature for coverages of $\Theta\sim0.5$ ML is reduced to ~20 °C. The melting temperature of the striped phase $(\Theta=0.27$ ML) has also been investigated by GIXD, in which we find that $T_M=100\pm5$ °C. These melting temperatures are all significantly higher than that found for bulk decanethiol,[24] $T_M=-26$ °C, as well as other physisorbed alkane monolayer systems.[25]

The existence of different stability regions has, of course, important consequences for the growth process. In Fig. 4, we plot the evolution of the two-dimensional coherence length (i.e., domain size) as a function of coverage (measured in real time during growth with GIXD). We find that there are two distinct types of behavior that occur as a function of the substrate temperature. In the high-temperature $(T>15$ °C) regime, the coherence length saturates at a substrate-limited ~2000 Å almost as soon as the $C(4\times2)$ phase is observed. This behavior is indicative of a high degree of molecular mobility during growth, and is characteristic of true equilibrium growth conditions. In contrast, at low temperatures $(T<15$ °C) the coherence length increases monotonically and slowly during growth and saturates at a significantly lower

value, which is instead indicative of a nonequilibrium growth process. Surprisingly, the evolution of the coherence length below 15 °C is *independent of the growth rate* in the regime studied (see Fig. 4), which demonstrates that surface diffusion and/or molecular reorganization are *not* rate-limiting processes in this regime.

The observed domain size evolution below 15 °C is well-described by a model (solid line, Fig. 4) in which a *fixed* number of islands grows monotonically in size. These observations, coupled with the equilibrium (Θ,T) phase diagram in Fig. 3, suggest that these two growth regimes are due to the presence or absence of a melted phase during growth.[26] Above 15 °C the liquid phase provides a medium for molecular exchange between islands allowing the islands to grow (e.g., through Ostwald ripening), while below this temperature no liquid phase is present, molecular exchange between islands is eliminated, and the islands are stable once formed. Therefore, it is the (Θ,T) phase behavior (and not diffusion or internal conformational changes) that provides the first deviation from ideal equilibrium growth behavior. The fact that the widely used room-temperature growth conditions are located in the higher temperature regime is possibly one reason that C10/Au(111) is a well-behaved, highly ordered, ''model'' SAM system.

It is interesting to note that it is the coverage-dependent melting behavior, $T_M(\Theta)$ (and specifically the large depression of the melting point for $\Theta<1$) that makes it possible to form highly ordered monolayers *even at room temperature*. That is, the intrinsic difference in thermodynamic stability between partially formed and completed structures allows the material to remain ''soft'' and responsive until just prior to completion, at which point it becomes more ''rigid'' and locked-in, as has been observed in the viscoelastic properties of the thiol/Au system.[13] This thermodynamic behavior is characteristic of many adsorbed systems [e.g., N_2/graphite, where $T_M(\Theta=1)=80$ K (Ref. 27)], where the melting point depression, $T_M(\Theta)$, has been shown to be related to the entropy of the high-temperature phase. The overall similarity to the behavior shown in Fig. 3 suggests that entropic contributions (e.g., from configurational entropy, and conformational entropy due to gauche defects) also play an important role in the SAM thermodynamics, and may be related to our observation of a liquid phase of *chemisorbed* thiol molecules at temperatures as low as ~ 20 °C (for $\Theta\sim 0.5$ ML). This also suggests that it may be possible to ''engineer'' the thermal response of these systems over a wide temperature range through changes in the entropic contributions due to ''rigidity'' of the molecular axis (i.e., increasing rigidity should result in increased thermal stability).

In summary, we have found that the primary difference between molecular self-assembly and the growth of ''simple'' (e.g., atomic) adsorbates is apparently in the multiple energy scales present in this system (due to physisorption, chemisorption, and molecule-molecule interactions), which are then reflected in numerous adsorption mechanisms, structures, and growth regimes. We expect that the detailed growth behavior will undoubtedly depend upon a range of variables such as the growth environment (e.g., with and without solvent), the molecular rigidity, and possibly even the headgroup-substrate chemistry. Yet, we expect that the richness and complexity that we report here for vapor deposited monolayers should be indicative of the *typical* behavior of this general class of materials, and underlines the need for molecular-level studies as the fundamental basis for understanding the growth processes in these systems.

Note Added in Proof. More extensive measurements of the initial nucleation and growth of C20/Au(111) has been performed with LEAD [P. Schwartz, F. Schreiber, P. Eisenberger,and G. Scoles (unpublished)].

We would like to acknowledge the generosity of M. Linford and C. E. D. Chidsey in providing purified thiols, as well as interactions with M. Bedzyk, and the experimental assistance provided by B. Karlin during the XPS measurements. This work was supported by the NSF (DMR 93-11871) and the DOE (DE-FG02-93ER45503), and F.S. was supported by the DFG (SCHR537/2-1). Some work was performed at the NSLS, which is supported by DOE Contract No. DE-AC0276CH-00016.

*Present address: Max-Planck Institut für Metallforschung, 70569, Stuttgart, Germany.

†Present address: Los Alamos National Laboratory, Los Alamos, NM 87544.

‡Present address: Argonne National Laboratory, ER-203, Argonne, IL 60439.

§Present address: Columbia Earth Institute, New York, NY 10027.

[1] A. Klug, Angew. Chem. Int. Ed. Engl. **22**, 565 (1983); H. Ringsdorf *et al.*, *ibid.* **27**, 113 (1988).

[2] G. M. Whitesides *et al.*, Science **254**, 1312 (1991).

[3] T. W. Bell, Science **271**, 1077 (1996).

[4] L. H. Dubois *et al.*, Annu. Rev. Phys. Chem. **43**, 437 (1992).

[5] A. Ulman, *An Introduction to Ultrathin Organic Films* (Academic, San Diego, 1991).

[6] G. E. Poirier *et al.*, Langmuir **10**, 3383 (1994).

[7] L. H. Dubois *et al.*, J. Chem. Phys. **98**, 678 (1993).

[8] N. Camillone III *et al.*, Langmuir **12**, 2737 (1995).

[9] A. Eberhardt, P. Fenter, and P. Eisenberger, Surf. Sci. Lett. (to be published).

[10] G. E. Poirier *et al.*, Science **272**, 1145 (1996). While real space images of the various growth stages are provided in this paper, the growth processes themselves are not quantitatively studied.

[11] M. Buck *et al.*, J. Vac. Sci. Technol. A **10**, 926 (1992).

[12] D. S. Karpovich *et al.*, Langmuir **10**, 3315 (1994).

[13] R. C. Thomas *et al.*, Langmuir **7**, 620 (1991).

[14] G. Hähner *et al.*, Langmuir **9**, 1955 (1993).

[15] K. A. Peterlinz *et al.*, Langmuir **12**, 4731 (1996).

[16] P. Fenter *et al.*, Phys. Rev. Lett. **70**, 2447 (1993).

[17] P. Fenter *et al.*, Science **266**, 1216 (1994).

[18] Since the data were obtained independently and the absolute exposures are not determined to better than a factor of ~ 3, we have corrected the exposure of the GIXD data by a factor of 2.8 for presentation. The absolute exposure was determined through the ion gauge reading by estimating that its sensitivity to decanethiol was a factor of 8.0 smaller than that of N_2; see for instance, R. L. Summers, NASA Technical Note No. TND-5285 (1969).

[19] Since we find below that the evolution of the monolayer involves three phases, one might expect on general grounds that the growth should exhibit three distinct time constants. Our results

suggest that two of the time constants are indistinguishable under these growth conditions.

[20] While we do not observe an ordered phase at these intermediate exposures, a disordered striped phase (Ref. 10), and a $5\sqrt{3} \times \sqrt{3}$ phase [Refs. 7, 8, and Gerlach *et al.*, Appl. Phys. A: Mater. Sci. Process. **65**, 375 (1997)] have been previously observed (with STM, LEAD, and LEED). These phases might be stabilized from the disordered ''intermediate'' phase under particular growth conditions as local minima in the free energy surface.

[21] M. Grunze, Phys. Scr. **T49B**, 711 (1993).

[22] S. M. Wetterer, D. J. Lavrich, S. L. Bernasek, and G. Scoles. Accepted in J. Phys. Chem. (1998).

[23] A. Eberhardt, Ph.D. thesis, Princeton University (1996). This coverage determination is independent of the calibration errors between the different systems, and requires only the knowledge of a two-step adsorption process (as shown by XPS) and the assumption that the surface remains covered during the conversion from the intermediate phase to the $C(4\times2)$ phase, as has been observed (Ref. 10).

[24] D. M. Small, *The Physical Chemistry of Lipids* (Plenum, New York, 1986).

[25] For instance, a ''lying down'' heptane monolayer on graphite melts at 140 K [H. Taub (private communications)].

[26] Other growth regimes may also be possible. For instance, others have observed [H.-G. Rubahn (private communications)], and we have confirmed with LEAD, that it may be possible to get kinetically trapped in the intermediate phases (see Ref. 20) above room temperature, and with relatively small fluxes. This behavior has not yet been systematically explored.

[27] B. Kuchta and R. D. Etters, Phys. Rev. B **54**, 12 057 (1996).